A Note on the Calculation of Supercavitating Hydrofoils With Rounded Noses[1]

O. FURUYA
A. J. ACOSTA
California Institute of Technology, Division of Engineering and Applied Science, Pasadena, Calif.

Practical supercavitating hydrofoils have rounded leading edges for mechanical strength. The prediction of pressures near the leading edge of such hydrofoils by linearized free-streamline theory fails because singularities are usually required there by the theory. A simple method based on singular perturbations of avoiding these difficulties for hydrofoils which have parabolic noses but an arbitrary profile downstream of the leading edge is presented. The results of such a computation on a hydrofoil with a parabolic profile and with fixed cavity separation near the leading edge radius are shown and are compared with an exact free-streamline theory. The agreement is excellent.

Introduction

Long cavities are often created downstream of vane sections in pumps, turbines, and on the components of modern high-speed hydrofoil craft.

Such supercavitating hydrofoils in practical use necessarily require some leading edge thickness to provide mechanical integrity. To design such a hydrofoil system it is important to predict not only the forces but also the pressure distribution on the body, particularly at off-design conditions.

Most exact analytical methods for solving streamline problems with arbitrary body profiles use the hodograph technique and variants in Levi-Civita's [1][2] original theory. Of these exact methods, one of the most salient proposals to appear recently is the functional iterative method of Wu and Wang [2]. In actual computations with this type of approach, numerical complexities and difficulties often arise owing to the computational instability inherent in this type of problem, and which is quite often experienced.

Many attempts were made to avoid the nonlinearity of the exact theory and also computational difficulties mentioned. Brodetsky [4], Oba [5], Larock and Street [6], and Murai and Kinoe [7] expressed the flow angle on the body (unknown as a function of potential a priori) by power series in potential. Larock and Street took only two such terms, while Murai and Kinoe incorporated leading edge curvature in those power series expansions. The coefficients in these power series are obtained by collocation of the flow angle or curvature on the body at discrete points. The final profile found as the result of a calculation cannot be determined in advance unless a very great number of terms in the series are used. We should mention, however, that these two groups of authors are the only ones who have successfully to date presented calculations of practical hydrofoils with blunt noses.

On the other hand, the linearized free-streamline theory of Tulin [8] is a simple and direct method to calculate the forces on thin bodies. Yet this theory fails to predict the pressure on the body except far away from the leading edge, because the theory itself requires singularities at the leading edge to represent a stagnation flow when such flow is present.

In view of the situation just outlined, it is very desirable to have a simple, direct, and accurate procedure which predicts the pressure distribution on the body for design purposes but without the complexities required of the truly exact methods.

Present Method

The approach adopted in the present work is that of singular perturbation theory. (See, for example, Van Dyke [9] and Cole [10].) As applied to the present problem, we assume that the angle of attack, camber, and body and cavity-thickness are "small." Far away from the leading edge perturbation velocities can then be considered to be small also, so that linearized free-streamline theory can be applied there. (This region of the flow is called the "outer region.") However, very near the leading edge (called the "inner region") there is a stagnation point and the body is highly curved; the linearized theory is evidently not valid in this region. This type of situation is made-to-order for the singular perturbation method as described in [9]. In the

[1] Presented at the Second International JSME Symposium, Fluid Machinery and Fluidics, Tokyo, Japan, 1972.

[2] Numbers in brackets designate References at end of paper.

Contributed by the Fluids Engineering Division and presented at the Winter Annual Meeting, New York, N. Y., November 26–30, 1972, of The American Society of Mechanical Engineers. Manuscript received at ASME Headquarters, August 1, 1972. Paper No. 72-WA/FE-28.

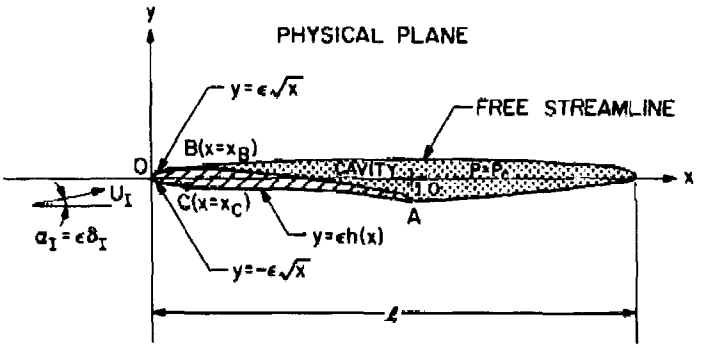

Fig. 1 Sketch showing an isolated supercavitating hydrofoil with a parabolic nose smoothly connected to an arbitrary profile shape

present case we seek to blend a local nonlinear "inner solution" smoothly to an "outer" linear solution. A considerable facility is afforded to this blending process if the inner solution is not too complex. A further simplifying feature of the present calculation is that accuracy greater than that of the linear theory far from the nose is not being sought. It seems reasonable, therefore, in the present circumstances to adopt the simplest possible nonlinear prescription for the inner flow that preserves the essential features of the problem. Such a flow is that around a parabola.

Two cases of this inner flow are considered: the first is for the case of the free-streamline detachment point far downstream of the leading edge. This is termed the "regular" case. In the second case, a free-streamline may appear within the vicinity of the leading edge radius (or inner region). This case is termed the "critical" case. The blending procedure is elementary for the regular case. As will be shown, it is possible to find a sufficiently accurate inner solution for the critical case to carry out the matching.

General Formulation

Consider the flow configuration as shown in Fig. 1, in which a parabolic nose defined by $y = \pm \epsilon\sqrt{x}$ is smoothly connected to an arbitrary lower profile shape of $y = \epsilon h(x)$ at an arbitrary point C, where ϵ is a small quantity. The angle of attack at upstream infinity is defined by the small quantity α_I, rewritten by $\epsilon\delta_I$ for notational convenience. Assuming the cavity pressure p_c to be constant, one can define cavitation number σ by the usual relation

$$\sigma = \frac{p_I - p_c}{\frac{1}{2}\rho U_I^2}$$

where p_I and U_I are the static pressure and flow speed at upstream infinity and ρ is the fluid density. The cavitation number is arbitrary but like the angle of attack is assumed to be small. In addition, the flow is assumed to be two-dimensional, steady, incompressible potential flow.

Outer Solution

In the present problem there are two independent small parameters, ϵ and σ. Without the perturbation expansions in both parameters, solutions of less accuracy are obtained for finite cavity length cases ($\sigma \neq 0$). (See, e.g., [3] and [8].) The expansions for u and v, therefore, are[3]

$$\frac{u}{U_c} = 1 + [\epsilon u_{1\epsilon} + \epsilon^2 u_{2\epsilon} + \ldots] + [\sigma u_{1\sigma} + \sigma^2 u_{2\sigma} + \ldots] \quad (1)$$

$$\frac{v}{U_c} = [\epsilon v_{1\epsilon} + \epsilon^2 v_{2\epsilon} + \ldots] + [\sigma v_{1\sigma} + \sigma^2 v_{2\sigma} + \ldots] \quad (2)$$

where u, v are the usual Cartesian velocity components and U_c, the flow speed on the cavity, is expressed by $U_c = U_I\sqrt{1+\sigma}$ using the Bernoulli equation. With the original form in mind, we rewrite (1) and (2) as follows:

$$\frac{u}{U_c} = 1 + \epsilon u_1 + \epsilon^2 u_2 + \ldots$$

$$\frac{v}{U_c} = \epsilon v_1 + \epsilon^2 v_2 + \ldots$$

where

$$u_n = u_{n\epsilon} + \left(\frac{\sigma}{\epsilon}\right)^n u_{n\sigma} \text{ and } v_n = v_{n\epsilon} + \left(\frac{\sigma}{\epsilon}\right)^n v_{n\sigma}.$$

The complex velocity function of first order is

$$w_1 = u_1 - iv_1.$$

The boundary conditions which u and v should satisfy are listed as follows:

(i) The flow is tangent to the body so that on the wetted part of the hydrofoil,

$$\frac{v}{u} = \left.\frac{dy}{dx}\right|_{\text{body}}.$$

(ii) The magnitude of the flow speed on the cavity is U_c, then

$$u^2 + v^2 = U_c^2.$$

(iii) At upstream infinity

$$u = U_I \cos\alpha_I = U_I \cos\epsilon\delta_I$$

$$v = U_I \sin\alpha_I = U_I \sin\epsilon\delta_I.$$

(iv) A cavity closure condition: We will require the body-cavity system to form a closed body although alternative schemes appear superior [11]. This condition can be expressed as

$$\oint_{\text{Body-Cavity (B.C.)}} dy = \oint_{\text{B.C.}} \frac{v}{u}\,dx = 0.$$

When the series expansions for u and v in (1) and (2) are substituted into these boundary conditions (i) ~ (iv) and are equated in like powers of ϵ and σ, the boundary conditions for u_1 and v_1

[3] Products of ϵ and σ should also appear in these expansions as noted by a reviewer, but they are not needed in the present linear theory, as he also observed.

Table 1 Linearized Boundary Conditions

	Boundaries in z-plane	$u_{1\epsilon}$ and/or $v_{1\epsilon}$	$u_{1\sigma}$ and/or $v_{1\sigma}$	u_1 and/or v_1 in (6)
	$0 < x < x_B,\ y = +0$	$v_{1\epsilon} = \dfrac{1}{2\sqrt{x}}$	$v_{1\sigma} = 0$	$v_1 = \dfrac{1}{2\sqrt{x}}$
(i) On the body	$0 < x < x_C,\ y = -0$	$v_{1\epsilon} = -\dfrac{1}{2\sqrt{x}}$	$v_{1\sigma} = 0$	$v_1 = -\dfrac{1}{2\sqrt{x}}$
	$x_C < x < 1,\ y = -0$	$v_{1\epsilon} = h'(x)$	$v_{1\sigma} = 0$	$v_1 = h'(x)$
(ii) On the cavity	$x_B < x < l,\ y = +0$ $1 < x < l,\ y = -0$	$u_{1\epsilon} = 0$	$u_{1\sigma} = 0$	$u_1 = 0$
	$z \to \infty$	$u_{1\epsilon} = 0$	$u_{1\sigma} = -\dfrac{1}{2}$	$u_1 = -\dfrac{\sigma}{2\epsilon}$
(iii) At infinity		$v_{1\epsilon} = \delta_I$	$v_{1\sigma} = 0$	$v_1 = \delta_I$
(iv) Closure condition	$\mathrm{Im}\oint_{\Gamma_z} w_1(z)dz = 0$			where Γ_z is a contour in clockwise direction as depicted in Fig. 2(a)

are found, as shown in the following Table 1 (note that velocity components away from the x-axis can be obtained by Taylor series expansions.)

We now apply standard methods of complex variable analysis for this outer problem. The linearized boundary conditions of Table 1 are shown in Fig. 2(a) where, in the complex z-plane, the hydrofoil-cavity system appears as a slit and x_B, the separation point, is assumed to be known (see Fig. 1). This slit is mapped onto the real axis of an auxiliary plane by the relation

$$\zeta = c\sqrt{\frac{-z}{z-l}} \tag{3}$$

where $c = \sqrt{l-1}$. The boundary conditions of Table 1 are also mapped onto this new plane (see Fig. 2(b)). We proceed to

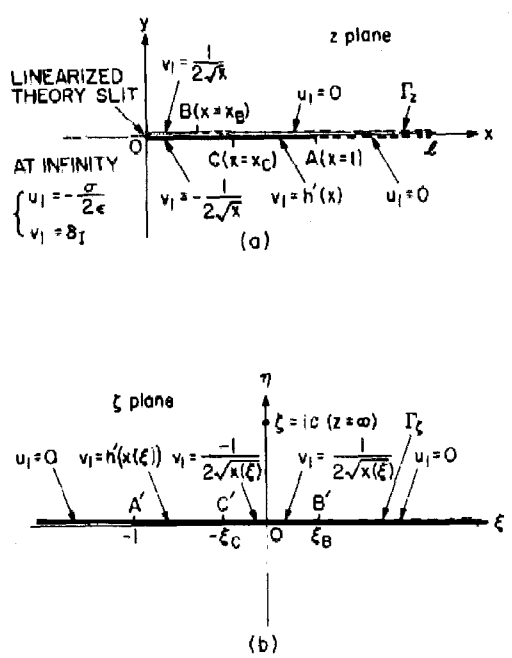

Fig. 2 Linearized boundary conditions for the complex velocity in the physical (z) and transform (ζ) planes

a solution by defining the new function $W_1 = iw_1$, and by making use of the analytic continuation $W_1(\bar{\zeta}) = \overline{W_1(\zeta)}$ have a problem treated in the now standard reference on this subject [12]. Introducing the notation,

$$W_1^+ = W_1(\xi, +0) = v_1(\xi, 0) + iu_1(\xi, 0)$$
$$W_1^- = W_1(\xi, -0) = v_1(\xi, 0) - iu_1(\xi, 0),$$

one can write the boundary conditions (i) to (iii) as

$$W_1^+ - W_1^- = 2iu_1(\xi, 0) = 0 \qquad \text{for } -\infty < \xi < -1$$
$$W_1^+ + W_1^- = 2v_1(\xi, 0) = 2h'(x(\xi)) \qquad \text{for } -1 < \xi < -\xi_C$$
$$W_1^+ + W_1^- = 2v_1(\xi, 0) = \frac{\sqrt{\xi^2 + c^2}}{\beta^{1/2}\xi} \qquad \text{for } -\xi_C < \xi < \xi_B$$
$$W_1^+ - W_1^- = 2iu_1(\xi, 0) = 0 \qquad \text{for } \xi_B < \xi < \infty$$

where the relation between x and ξ in equation (3) has been used. Under the conditions that the velocity be finite at the trailing edge and that $w_1(z)$ behave like $1/\sqrt{z-l}$ as $z \to l$, the unique solution to this problem is:

$$W_1(\zeta) = \sqrt{(\zeta+1)(\zeta-\xi_B)}\left\{\frac{1}{2\pi i}\right.$$
$$\oint_{-1}^{-\xi_C} \frac{2h'(x(\xi'))}{i\sqrt{(1+\xi')(\xi_B-\xi')}}\,\frac{d\xi'}{\xi'-\zeta} + \frac{1}{2\pi i}$$
$$\left.\int_{-\xi_C}^{\xi_B} \frac{\sqrt{\xi'^2+c^2}}{i\beta^{1/2}\xi'\sqrt{(1+\xi')(\xi_B-\xi')}}\,\frac{d\xi'}{\xi'-\zeta} + A_1 + \frac{B_1}{\zeta}\right\} \tag{4}$$

where A_1, B_1, and the length of cavity l are unknown real constants. These quantities are determined by the boundary condition (iii) and the closure condition (iv) of Table 1. (iii) gives

$$\delta_I + i\left(-\frac{\sigma}{2\epsilon}\right) = W_1(ic) \tag{5}$$

where $\zeta = ic$ corresponds to the infinity in z-plane, and (iv) gives

$$\operatorname{Im}\oint_{\text{B.C.}} w_1(z)dz = \operatorname{Im}\oint_{\Gamma_z} w_1(z)dz = -\operatorname{Re}\int_{\Gamma_\zeta} W_1(\zeta)\frac{dz}{d\zeta}d\zeta = 0 \tag{6}$$

where Γ_ζ is the contour in ζ-plane, which corresponds to Γ_z.

Three relations obtained from equations (5) and (6) can be written in a matrix form and then explicitly solved for A_1, B_1, and σ, i.e.,

$$\begin{bmatrix} 0 & m_{12} & m_{13} \\ 1/2\epsilon & m_{22} & m_{23} \\ 0 & m_{32} & m_{33} \end{bmatrix} \begin{bmatrix} \sigma \\ A_1 \\ B_1 \end{bmatrix} = \begin{bmatrix} N_1 \\ N_2 \\ N_3 \end{bmatrix}. \tag{7}$$

The coefficients m_{ij}, N_i are all real constants and defined by the equations

$$m_{12} + im_{22} = J_1(ic),\ m_{13} + im_{23} = J_2(ic)$$

$$m_{32} = \operatorname{Re}\left\{\int_{\Gamma_\zeta} J_1(\zeta)\frac{dz}{d\zeta}d\zeta\right\},\ m_{33} = \operatorname{Re}\left\{\int_{\Gamma_\zeta} J_2(\zeta)\frac{dz}{d\zeta}d\zeta\right\}$$

$$N_2 = \delta_I - \operatorname{Re}\{I_0(ic)\},\ N_3 = -\operatorname{Im}\{I_0(ic)\}$$

$$N_3 = -\operatorname{Re}\left\{\int_{\Gamma_\zeta} I_0(\zeta)\frac{dz}{d\zeta}d\zeta\right\}$$

and

$$J_1(\zeta) = \sqrt{(\zeta+1)(\zeta-\xi_B)},\ J_2(\zeta) = \frac{J_1(\zeta)}{\zeta},$$

$$I_0(\zeta) = \frac{J_1(\zeta)}{2\pi i}\left(\int_{-1}^{-\xi_C}\frac{2h'(x(\xi'))}{i\sqrt{(1+\xi')(\xi_B-\xi')}}\frac{d\xi'}{\xi'-\zeta} + \int_{-\xi_C}^{\xi_B}\frac{\sqrt{\xi'^2+\epsilon^2}}{i\epsilon/2\xi'\sqrt{(1+\xi')(\xi_B-\xi')}}\frac{d\xi'}{\xi'-\zeta}\right).$$

These equations provide a formal solution to the outer problem. The velocity profile on the body then can be written to the first order as

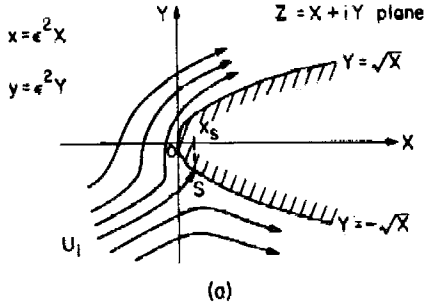

(a)

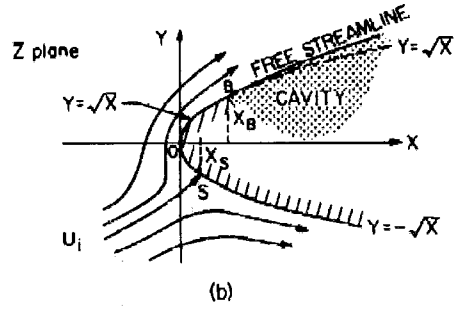

(b)

Fig. 3 Sketch showing the inner flow about the basic parabola; (a) shows the regular case and (b) shows the critical case in which a free streamline appears

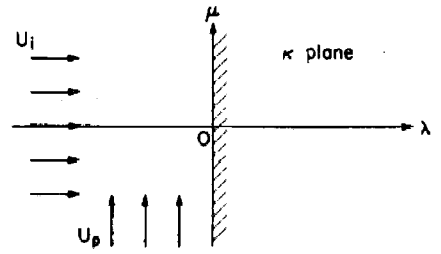

Fig. 4 Transform plane ($Z = \kappa - \kappa^3$) for the solution of the regular inner flow

$$\frac{q_0}{U_e} = 1 + \epsilon u_1\Big|_{\text{body}} + O(\epsilon^2) \tag{8}$$

where

$$u_1\Big|_{\text{body}} = \operatorname{Im}\{W_1(\xi, +0)\} \text{ for } -1 < \xi < \xi_B.$$

Inner Solution

The outer solution obtained in equation (8) has singularities at the leading edge and the series expansions of the velocities then are not valid for $\xi = O(\epsilon)$ or $x = O(\epsilon^2)$. Following the methods of [9], we are led to consider an inner region stretched by the factor ϵ^2, i.e.,

$$x = \epsilon^2 X,\ y = \epsilon^2 Y \tag{9}$$

X, Y being the coordinates in the inner region. Within this inner region we have the two cases previously mentioned:

A. Regular Case. The local flow configuration is now shown in Fig. 3(*a*). By the mapping function $Z = \kappa - \kappa^3$, the flow field in the z-plane is mapped onto the left half κ-plane as shown in Fig. 4. The complex velocity potential W_i for the flow around the infinite parabola in the κ-plane is readily found as

$$W_i = W_s + W_p$$

where W_s and W_p are that of a stagnation flow and of a parallel flow, respectively, or

$$W_i = -U_i\kappa^2 - iU_p\kappa$$

where U_i and U_p are unknown constants. Since the velocity q_i is given by $(dW_i/dZ \cdot \overline{dW_i/dZ})^{1/2}$, q_i on the body is found to be

$$\frac{q_i}{U_i} = \sqrt{\frac{X}{1/4+X}}\left|1 \pm \frac{b}{X^{1/2}}\right|,$$

which, in terms of unstretched coordinates, is

$$\frac{q_i}{U_i} = \sqrt{\frac{x}{\epsilon^2/4+x}}\left|1 \pm \frac{\epsilon b}{x^{1/2}}\right| \tag{10}$$

where U_i and b are two unknown parameters representing the magnitude of the local uniform flow speed and the location of the stagnation point, respectively. In these equations the upper sign is for the upper portion of the body and the lower sign for the lower portion.

B. Critical Case. This is the case in which the upper cavitation separation point is fixed near the leading edge and a free-streamline then appears in the inner region, as depicted in Fig. 3(*b*). In order to solve this nonlinear problem analytically, we assume that the upper free-streamline is approximated by the nose shape $Y = \sqrt{X}$, so that the body-cavity boundary can be mapped onto a straight line again. The mapping function for this purpose is given by $Z = i\kappa + \kappa^2$, and the flow field, therefore, is mapped onto the upper half of the κ-plane, as shown in Fig. 5. We define the hodograph variable ω_i by the equation

$$\frac{dW_i}{d\Omega} = q_i e^{i\theta} = U_i e^{i\omega_i} \tag{11}$$

then

$$\omega_i = \theta + i\tau, \tau = \ln\frac{q_i}{U_i}.$$

With the analytical continuation of ω_i into the lower half of the κ-plane by $\omega_i(\bar{\kappa}) = \overline{\omega_i(\kappa)}$, one has the boundary value problem

$$\omega_i^+ + \omega_i^- = 2\theta_0 \text{ for } -\infty < \lambda < \lambda_B$$

$$\omega_i^+ - \omega_i^- = 0 \quad \text{for } \lambda_B < \lambda < \infty$$

where θ_0 is the flow angle on the wetted body. The unique solution to this problem is

$$\omega_i(\kappa) = \tan^{-1}\frac{1}{2\kappa} + i\ln\frac{-\lambda_S - \kappa}{(\sqrt{\lambda_B + \lambda_S} + \sqrt{\lambda_B - \kappa})^2} \times \left(\frac{R_0 + (\lambda_B - \kappa) + 2R_0^{1/2}\sin\frac{\theta_0}{2}\cdot\sqrt{\lambda_B - \kappa}}{R_0 + (\lambda_B - \kappa) - 2R_0^{1/2}\sin\frac{\theta_0}{2}\cdot\sqrt{\lambda_B - \kappa}}\right)^{1/2}.$$

From the definition given in equation (11), the velocity q_i on the body is given by square root of $U_i^2 e_i^{\omega_i}\cdot e^{-i\overline{\omega_i}}$. Then

$$\frac{q_i}{U_i} = \frac{\left|\lambda_S \pm \frac{x^{1/2}}{\epsilon}\right|}{\left(\sqrt{\frac{x_B^{1/2} \mp x^{1/2}}{\epsilon}} + \sqrt{\frac{x_B^{1/2}}{\epsilon} + \lambda_S}\right)^2} \times \left(\frac{R_0 + \left(\frac{x_B^{1/2} \mp x^{1/2}}{\epsilon}\right) + 2R_0^{1/2}\sin\frac{\theta_0}{2}\cdot\sqrt{\frac{x_B^{1/2} \mp x^{1/2}}{\epsilon}}}{R_0 + \left(\frac{x_B^{1/2} \mp x^{1/2}}{\epsilon}\right) - 2R_0^{1/2}\sin\frac{\theta_0}{2}\cdot\sqrt{\frac{x_B^{1/2} \mp x^{1/2}}{\epsilon}}}\right)^{1/2} \tag{12}$$

where

$$R_0 = \left(\frac{x_B}{\epsilon^2} + \frac{1}{4}\right)^{1/2} \text{ and } \theta_0 = \pi + \tan^{-1}\left(\frac{-\epsilon}{2x_B^{1/2}}\right) \tag{13}$$

and U_i and λ_S are unknown parameters of the same meaning as those in regular cases.

It should be mentioned that equation (12) is not an exact solution but its error is less than $\epsilon^{3/2}$ [13].

Matching

The suggested method for matching these equations [9] is to expand the outer solution in the inner variable X and the inner solution is to be expanded in the outer valuable x; the constants are adjusted so that the solutions match each other to the same order of ϵ. The first two leading terms of equation (8) after expansion and needed for matching are:

regular case,

$$\frac{q_0}{U_e} = 1 + \epsilon B_1\frac{\sqrt{\xi_B}}{\xi}$$

or, with equation (3),

$$\frac{q_0}{U_e} = 1 \pm \epsilon B_1\frac{\sqrt{l\xi_B}}{c}\frac{1}{x^{1/2}} \tag{14}$$

and for the *critical case*

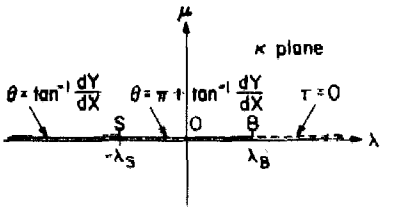

Fig. 5 Boundary conditions for the hodograph variable $\omega = \theta + i\tau$ in the transform plane to obtain the solution for the critical inner flow

$$\frac{q_0}{U_e} = 1 + \epsilon B_1\frac{\sqrt{\xi_B - \xi}}{\xi} = 1 - \epsilon B_1\frac{\pi^{1/4}}{c^{1/2}}\frac{\sqrt{x_B^{1/2} + x^{1/2}}}{x^{1/2}}. \tag{15}$$

The inner expansions are:

regular case,

$$\frac{q_i}{U_i} = 1 \pm \frac{\epsilon b}{x^{1/2}} \tag{16}$$

from equation (10) and for the *critical case*

$$\frac{q_i}{U_i} = 1 - \epsilon^{1/2}\left(2\sqrt{\frac{x_B^{1/2}}{\epsilon} + \lambda_S} - 2R_0^{1/2}\sin\frac{\theta_0}{2}\right)\frac{\sqrt{x_B^{1/2} + x^{1/2}}}{x^{1/2}} \tag{17}$$

from equation (12). Matching now requires that

$$U_i = U_e, b = B_1\frac{\sqrt{l\xi_B}}{c} \tag{18}$$

for the *regular case* and

$$U_i = U_e, 2\sqrt{\frac{x_B^{1/2}}{\epsilon} + \lambda_S} - 2R_0^{1/2}\sin\frac{\theta_0}{2} = \epsilon^{1/2}B_1\frac{\pi^{1/4}}{c^{1/2}} \tag{19}$$

for the *critical case.*

Uniformly Valid Solutions

A simple way to construct a uniformly valid solution is to add the inner and outer solution and to subtract the common part. The common parts are given by equations (14) and (15) for the regular and critical cases, respectively. These solutions are:

regular case,

$$\frac{q}{U_e} = \sqrt{\frac{x}{\epsilon^2/4 + x}}\left|1 \pm \frac{\epsilon b}{x^{1/2}}\right| + \epsilon\sqrt{(1 + \xi(x))(\xi_B - \xi(x))} \times \left\{-\frac{1}{\pi}\int_{-1}^{-\xi_C}\frac{h'(x(\xi'))}{\sqrt{(1 + \xi')(\xi_B - \xi')}}\frac{d\xi'}{\xi' - \xi} - \frac{1}{2\pi l^{1/2}}\int_{-\xi_C}^{\xi_B}\frac{\sqrt{\xi'^2 + c^2}}{\xi'\sqrt{(1 + \xi')(\xi_B - \xi')}}\frac{d\xi'}{\xi' - \xi} + A_1\right\} + \epsilon B_1\left[\frac{\sqrt{(1 + \xi(x))(\xi_B - \xi(x))}}{\xi(x)} \mp \frac{\sqrt{l\xi_B}}{cx^{1/2}}\right] + O(\epsilon^2) \tag{20}$$

where A_1, B_1, b, c are given by equations (7), (18), and (3) in which the upper and lower signs are for the upper and lower portions of the body, respectively.

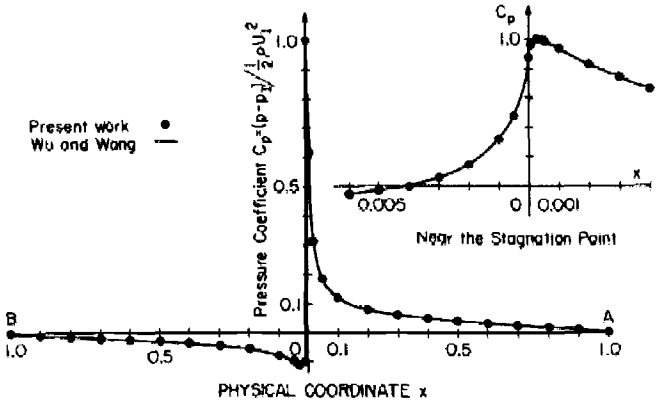

Fig. 6 Pressure distribution on a base ventilated, ($x_B = 1.0$), parabolic strut with $\epsilon = 0.1$ at zero cavitation number at one degree angle of attack. The calculations of the present work give a drag coefficient based on a chord of $C_D = 0.0152$ and a lift coefficient $C_L = 0.0494$. The exact values are 0.0148 and 0.0478, respectively.

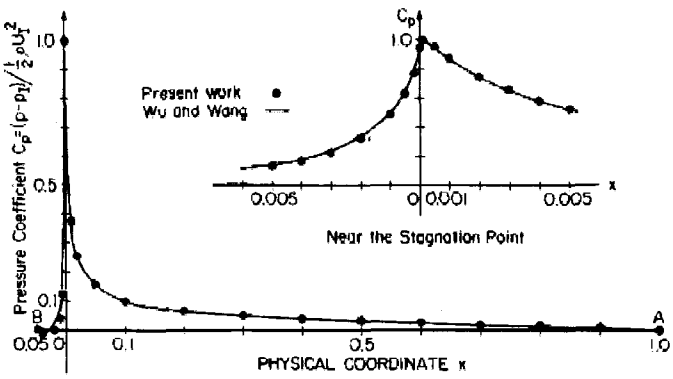

Fig. 7 Pressure distribution on the parabolic strut of Fig. 6 with cavity detachment at $x_B = 0.05$. The present method gives $C_D = 0.0189$, $C_L = 0.0521$, exact values being 0.0182, 0.0470, respectively.

critical case,

$$\frac{q}{U_c} = \frac{\left|\lambda_S \pm \frac{x^{1/2}}{\epsilon}\right|}{\left(\sqrt{\frac{x_B^{1/2} \mp x^{1/2}}{\epsilon}} + \sqrt{\frac{x_B^{1/2}}{\epsilon}} + \lambda_S\right)^2} \times \left(\frac{R_0 + \frac{x_B^{1/2} \mp x^{1/2}}{\epsilon} + 2R_0^{1/2}\sin\frac{\theta_0}{2}\cdot\sqrt{\frac{x_B^{1/2} \mp x^{1/2}}{\epsilon}}}{R_0 + \frac{x_B^{1/2} \mp x^{1/2}}{\epsilon} - 2R_0^{1/2}\sin\frac{\theta_0}{2}\cdot\sqrt{\frac{x_B^{1/2} \mp x^{1/2}}{\epsilon}}}\right)^{1/2}$$

$$+ \epsilon\sqrt{(1+\xi(x))(\xi_B - \xi(x))}\left\{-\frac{1}{\pi}\int_{-1}^{-\xi_C}\frac{h'(x(\xi'))}{\sqrt{(1+\xi')(\xi_B - \xi')}}\times\frac{d\xi'}{\xi' - \xi} - \frac{1}{2\pi l^{1/2}}\int_{-\xi_C}^{\xi_B}\frac{\sqrt{\xi'^2 + c^2}}{\xi'\sqrt{(1+\xi')(\xi_B - \xi')}}\frac{d\xi'}{\xi' - \xi} + A_1\right\}$$

$$+ \epsilon B_1\left[\frac{\sqrt{(1+\xi(x))(\xi_B - \xi(x))}}{\xi} \mp \frac{l^{1/4}\sqrt{x_B^{1/2} \mp x^{1/2}}}{c^{1/2}\, x^{1/2}}\right]$$

$$+ O(\epsilon^{3/2}) \qquad (21)$$

where A_1, B_1, λs, b, c, R_0, θ_0 are given by equations (7), (19), (3). and (13). Notice that there are no singularities in these solutions near the nose.

Special Cases

In the present work we treat a parabolic strut with an infinite cavity. The solutions reduce to

regular case,

$$\frac{q}{U_c} = \sqrt{\frac{x}{\epsilon^2/4 + x}}\left|1 \pm \frac{\epsilon\delta_I x_B^{1/4}}{x^{1/2}}\right|$$

$$\pm \frac{\epsilon\delta_I}{x^{1/2}}\left(\sqrt{(1 \pm x^{1/2})(x_B^{1/2} \mp x^{1/2})} - \sqrt{x_B^{1/2}}\right) + O(\epsilon^2) \qquad (20')$$

critical case,

$$\frac{q}{U_c} = \frac{\left|\lambda_S \pm \frac{x^{1/2}}{\epsilon}\right|}{\left(\sqrt{\frac{x_B^{1/2} \mp x^{1/2}}{\epsilon}} + \sqrt{\frac{x_B^{1/2}}{\epsilon}} + \lambda_S\right)^2} \times \left(\frac{R_0 + \frac{x_B^{1/2} \mp x^{1/2}}{\epsilon} + 2R_0^{1/2}\sin\frac{\theta_0}{2}\cdot\sqrt{\frac{x_B^{1/2} \mp x^{1/2}}{\epsilon}}}{R_0 + \frac{x_B^{1/2} \mp x^{1/2}}{\epsilon} - 2R_0^{1/2}\sin\frac{\theta_0}{2}\cdot\sqrt{\frac{x_B^{1/2} \mp x^{1/2}}{\epsilon}}}\right)^{1/2} \pm$$

$$\frac{\epsilon\delta_I}{x^{1/2}}\left(\sqrt{(1 \pm x^{1/2})(x_B^{1/2} \mp x^{1/2})} - \sqrt{x_B^{1/2} \mp x^{1/2}}\right) + O(\epsilon^{3/2}) \qquad (21')$$

where now

$$\lambda_S = \frac{1}{4}\left(\epsilon^{1/2}\delta_I + 2R_0^{1/2}\sin\frac{\theta_0}{2}\right)^2 - \frac{x_B^{1/2}}{\epsilon}.$$

Results

A number of cases with different location of a fixed cavity detachment point have been calculated for the supercavitating flow past a parabolic foil at zero cavitation number. The base of the foil is 20 percent of the chord ($\epsilon = 0.1$) and the angle of attack is fixed at one degree. These are presented in Figs. 6–9 together with calculations we have made using an exact theory due to Wu and Wang. It can be seen that the present approximate method gives excellent agreement for all cases except for the very last one, for which the detachment point is right on the nose itself. (The error in this latter case is on the order of $\epsilon^{3/2}$, which is not large.) The present method is not expected to give an accurate answer in this case because the free-streamline would not be expected to lie near the approximating parabola

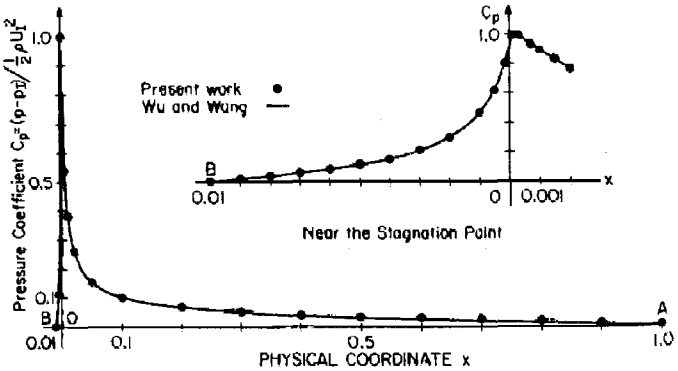

Fig. 8 Pressure distribution on the parabolic strut of Fig. 6 with cavity detachment at $x_B = 0.01$. The present method gives $C_D = 0.0191$, $C_L = 0.0547$ with corresponding exact values of 0.0186, 0.0511.

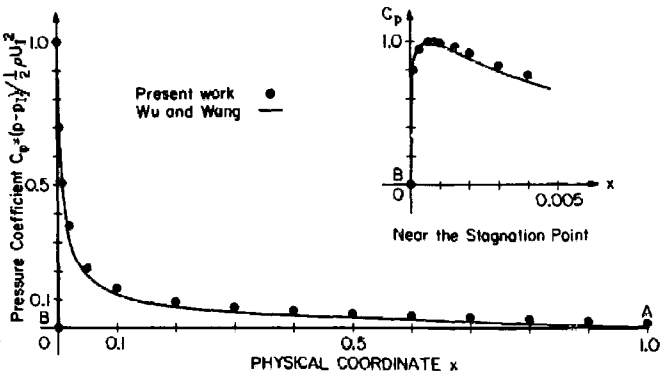

Fig. 9 Pressure distribution on the parabolic strut of Fig. 6 with cavity detachment at the nose itself ($x_B = 0.0$). The present method gives $C_D = 0.0193$, $C_L = 0.0762$ with corresponding exact values of 0.0167 and 0.0594.

of Fig. 3(*b*). Even, however, including this critical case, quite good accuracy is achieved.

Discussion

The present method relies on an inner solution that is not exact (for the critical case) and, as a consequence, "smooth" cavity separation cannot mathematically be insured to accuracies greater than that of the method itself. The separation is therefore strictly of the "fixed" type. However, for all practical purposes the occurrence of smooth separation can be determined by inspection of the numerical results. In any case, smooth separation is hardly found in practice on cavitating bodies so this point is perhaps academic. We should also like to mention that nose shapes other than parabolic could be chosen at the expense of complexity. Again, simplicity in the inner solution would require that, in the critical case, the local free-streamline would be well approximated by the shape chosen. When this is not the case, or when the angle of attack is large, we feel that it is better to proceed directly to a full nonlinear solution [e.g., (2), (4)] than to work out cumbersome higher approximations.

A great many additional applications of the present method have been made to isolated hydrofoils and to cascades of hydrofoils having arbitrary camber and cavitation number [13], and we hope to present these in the near future at an occasion as auspicious as the present one.

Finally, we should like to make a brief comment on the numerical work involved in the application of reference [2]. This requires the solution of a highly nonlinear integral equation and divergent solutions are often encountered in this type of problem. In the present calculations great care was given to the starting basic flow, a weighted iteration scheme was used, double precision was found to be required, and the spatial integration increments were varied in regions of rapid change. Each of these features was crucial in obtaining convergence, and this no doubt accounts for the lack of success in Lurye's calculations [14]. There is a further practical point: The computing time required on an IBM 370 was at least two orders of magnitude greater for the exact calculations than for the present method. Because of its simplicity, economy, and direct approach the present method should be useful for design purposes.

Acknowledgments

This work was supported by the Office of Naval Research under contract N00014-67-A-0094-0021. We also appreciate the interest and advice of Prof. Y. T. Wu and the helpful comments of the reviewers.

References

1 Levi-Civita, T., "Scie e leggi di resistenzia," *R. C. cir mat.*, Palermo, Vol. 18, 1907, pp. 1–37.
2 Wu, Y. T., and Wang, D. P., "A Wake Model for Free-Streamline Flow Theory, Part 2. Cavity Flows Past Obstacles of Arbitrary Profile," *Journal of Fluid Mechanics*, Vol. 18, 1963, pp. 65–93.
3 Wu, Y. T., "Note on the Linear and Nonlinear Theories for Fully Cavitated Hydrofoils," California Institute of Technology Rep. 21-22, 1956.
4 Brodetsky, S., "Discontinuous Fluid Motion Past Circular and Elliptic Cylinders," *Proceedings of the Royal Society of London*, A102, 1922, pp. 542–553.
5 Oba, R., "Theory for Supercavitating Flow Through an Arbitrary Hydrofoil," JOURNAL OF BASIC ENGINEERING, TRANS. ASME, Series D, Vol. 86, No. 2, June 1964, pp. 285–290.
6 Larock, B. E., and Street, R. L., "Cambered Bodies in cavitating flow—A Nonlinear Analysis and Design Procedure," *Journal of Ship Research*, Vol. 9, 1968, pp. 1–13.
7 Murai, H., and Kinoe, T., "Theoretical Research on Blunt-Nosed Hydrofoil in Fully Cavitating Flow," *Reports of the Institute of High Speed Mechanics*, Japan, Vol. 20, 1968/69.
8 Tulin, M. P., "Steady Two-Dimensional Cavity Flows About Slender Bodies," DTMB Rep. 834, 1953. Navy Dept., Washington, D. C.
—. "Supercavitating Flows—Small Perturbation Theory," *Journal of Ship Research*, Vol. 7, 1964, pp. 16–37.
9 Van Dyke, M., *Perturbation Methods in Fluid Mechanics*, Academic Press, New York, 1964.
10 Cole, J. D., *Perturbation Methods in Applied Mathematics*, Blaisdel, U.S.A., 1968.
11 Nishiyama, T., and Ota, T., "Linearized Potential Flow Models for Hydrofoils in Supercavitating Flows," JOURNAL OF BASIC ENGINEERING, TRANS. ASME, Vol. 93, Series D, No. 2, June 1971, pp. 550–564.
12 Muskhelishvili, N. I., *Singular Integral Equations*, Noordhoff, Gronigen, Holland, 1946.
13 Furuya, O., "A Singular Perturbation Method of Calculating the Behavior of Supercavitating Hydrofoils With Rounded Noses," PhD Thesis, California Institute of Technology, Pasadena, Calif., 1972.
14 Lurye, J. R., "Numerical Aspects of Wu's Method for Cavitated Flow, as Applied to Sections Having Rounded Noses," TRG-156-SR-3, Melville, N. Y., 1966.

DISCUSSION

W. B. Morgan[4]

The authors are to be congratulated on being able to obtain a solution to such a difficult problem. It seems to me that still unknown is the location of the cavity separation point on the foil suction side. Do the authors have any comments on how this point can be determined in a real fluid?

[4]Naval Ship Research and Development Center, Bethesda, Md.

Authors' Closure

The determination of the cavity separation point which is fixed in advance in the present work is an important part of the real cavitating flow problem, as pointed out by Dr. Morgan; yet there is no analytical method so far to solve this problem. So-called "smooth separation" condition is a mathematical criterion to fix the cavity separation point on smooth bodies, but the recent experimental study [15][5] has shown that this criterion does not predict the cavity separation point accurately. In order to accomplish this type of prediction more thorough investigation must be made by taking into account the real fluid effects such as viscosity, surface tension, nuclei and so on. In

[5]Numbers 15–16 designate Additional References at end of closure.

the recent work done by V. Arakeri [16] such a semiempirical method has been proposed to predict the separation point of a certain type of cavity based on the laminar boundary separation theory and experimental data of axisymmetric cavitating bodies, showing a new direction to this type of problem. Apparently, much more elaborate, both analytical and experimental work will be required in the future before a handy tool to predict the cavity separation point in a real fluid will be provided. Meanwhile, the accurate prediction of the pressure distribution is the first thing to be achieved in the cavity flow and the result will be very useful for design purposes including the determination of the cavity separation point.

Additional References

15 Brennen, C., *Cavitation State of Knowledge*, ASME, New York, 1969, p. 141.

16 Arakeri, V. H., "Viscous Effects in Inception and Development of Cavitation on Axi-Symmetric Bodies," California Institute of Technology, Rep. Eng. 183-1, 1973.